



Publication Year	2017
Acceptance in OA	2020-09-10T10:30:08Z
Title	X-ray orbital modulation of a white dwarf accreting from an L dwarf. The system SDSS J121209.31+013627.7
Authors	Stelzer, B., DE MARTINO, Domitilla, Casewell, S. L., Wynn, G. A., Roy, M.
Publisher's version (DOI)	10.1051/0004-6361/201630038
Handle	http://hdl.handle.net/20.500.12386/27279
Journal	ASTRONOMY & ASTROPHYSICS
Volume	598

LETTER TO THE EDITOR

X-ray orbital modulation of a white dwarf accreting from an L dwarf

The system SDSS J121209.31+013627.7

B. Stelzer¹, D. de Martino², S. L. Casewell³, G. A. Wynn³, and M. Roy³

¹ INAF–Osservatorio Astronomico di Palermo, Piazza del Parlamento 1, 90134 Palermo, Italy
e-mail: stelzer@astropa.inaf.it

² INAF–Osservatorio Astronomico di Capodimonte, Salita Moiariello 16, 80131 Napoli, Italy

³ Department of Physics and Astronomy, University of Leicester, Leicester, LE1 7RH, UK

Received 10 November 2016 / Accepted 5 January 2017

ABSTRACT

In an *XMM-Newton* observation of the binary SDSS J121209.31+013627.7, consisting of a white dwarf and an L dwarf, we detect X-ray orbital modulation as proof of accretion from the substellar companion onto the magnetic white dwarf. We constrain the system geometry (inclination as well as magnetic and pole-cap angle) through modelling of the X-ray light curve, and we derive a mass accretion rate of $3.2 \times 10^{-14} M_{\odot}/\text{yr}$ from the X-ray luminosity ($\sim 3 \times 10^{29}$ erg/s). From X-ray studies of L dwarfs, a possible wind driven from a hypothesized corona on the substellar donor is orders of magnitude too weak to explain the observed accretion rate, while the radius of the L dwarf is comparable to its Roche lobe ($0.1 R_{\odot}$), making Roche-lobe overflow the likely accretion mechanism in this system.

Key words. X-rays: binaries – accretion, accretion disks – stars: individual: SDSS J121209.31+013627.7 – white dwarfs – brown dwarfs

1. Introduction

Sensitive wide-field surveys such as SDSS and UKIDSS have boosted the number of known white dwarf (WD) main-sequence (MS) binaries. In the majority of these systems the non-degenerate component is an M dwarf.

Over 2000 systems consisting of a WD and an M dwarf (henceforth WDMD binaries) are known (Rebassa-Mansergas et al. 2013), but only about a dozen binaries that consist of a WD and an L dwarf (WDLB binaries; see Sect. 3 for accreting systems and Casewell 2014, for a summary of detached systems). This might be due to the difficulty of detecting such faint very late-type companions in the spectral energy distribution (SED) of WDs.

Similar to their higher-mass siblings, the WDMD binaries, the WDLB systems comprise both wide (separation tens to thousands of AU) and close binaries (period < 10 h). Only a handful of them are close systems (period ~ 100 min) in which the low-mass companion must have survived a common-envelope phase (Nordhaus & Spiegel 2013). The progenitors of wide systems composed of WD and brown dwarf (BD), the AU-scale BD-MS binaries, are also rarely discovered, and they define the so-called “brown dwarf desert” (Marcy & Butler 2000), suggesting that systems composed of WD and BD form rarely. However, the much more frequent WDMD binaries evolve into cataclysmic variables (CVs), and subsequently, both the binary separation and the donor mass decrease over time, which converts the donor into a close-in substellar object.

When the donor star leaves thermal equilibrium and starts to expand in response to its mass loss, the orbital evolution of a CV reverses. The period minimum that represents this change is observed and theoretically predicted to be at $P_{\text{orb}} \sim 82$ min

(Gänsicke et al. 2009; Knigge et al. 2011), corresponding to a donor mass of $\sim 0.06 M_{\odot}$. This means that the systems that have evolved beyond the period minimum, so-called period-bouncers, have a substellar donor. Binary population synthesis revealed that period-bouncing WDLB binaries are expected to be the greater portion ($\sim 70\%$) of the whole CV population (Howell et al. 2001). The predicted high abundance of such systems is at odds with the very low detection rate. Systems with a very low-mass companion are difficult to identify because the contrast between the WD and L dwarf at optical and infrared wavelengths is low. Only a few binaries composed of a WD and a BD are confirmed spectroscopically.

The type of binary interaction in close WD/MS systems is tied to the evolutionary state. During the CV phase, accretion occurs through Roche-lobe overflow, while in detached systems wind accretion may take place. A handful of systems showing very weak mass accretion ($< 10^{-13} M_{\odot}/\text{yr}$, e.g. Schmidt et al. 2007) were defined as low accretion rate polars (LARPs; Schwöpe et al. 2002). However, in most of them the donor is underfilling its Roche lobe, meaning that they are in a pre-CV phase, and they must be accreting from a wind (Schwöpe et al. 2009). Magnetic siphons that channel the entire wind of the donor onto the WD have been proposed to explain this class of systems with a strongly magnetic WD but weak or absent X-ray emission (Webbink & Wickramasinghe 2005).

Accretion rates of WD binaries can be inferred from the X-ray luminosity or from the broad-band UV to optical/near-IR spectral energy distribution (SED) arising from the accretion disk. $H\alpha$ emission provides only an upper limit to the accretion rate, since this line can also have a significant contribution from the donor star’s chromospheric activity or its irradiation by the WD. For the same reason, detection of X-rays at low levels

($L_x \leq 10^{29}$ erg/s) from WD binaries with M-dwarf donors is not sufficient to diagnose accretion. However, magnetic activity drops sharply at late-M spectral types (e.g. West et al. 2004), and the coronal X-ray emission levels of L dwarfs are generally below the current sensitivity limits (Stelzer et al. 2006). Only one very nearby L dwarf has been detected in X-rays so far, at a level of $\log L_x$ [erg/s] = 25.4 (Audard et al. 2007). Therefore, an X-ray detection of a WDL binary clearly points at accretion, whether through wind or Roche-lobe overflow. Only one short-period WDL system has been detected as X-ray emitter so far, SDSS J121209.31+013627.7 (SDSS 1212), which has been reported as a weak *Swift* source by Burleigh et al. (2006).

SDSS 1212 is a magnetic WDL binary (spectral type DA + L5/L8) with an average field strength of 7 MG (Schmidt et al. 2005; Farihi et al. 2008). Schmidt et al. (2005) found narrow H α emission with periodic radial velocity variation ($P \sim 90$ min) and large amplitude consistent with an origin in the L dwarf’s irradiated atmosphere. Photometric variability at the same period and roughly in anti-phase with the H α emission also indicates that there is a hot spot on the WD surface (Burleigh et al. 2006). The K_s -band light curve was shown by Debes et al. (2006) to be more consistent with cyclotron emission from a magnetic pole than with irradiation of a companion star. The authors also noted a clear excess in the H and K_s bands with respect to the expected SED of the WD, which was spectroscopically confirmed by Farihi et al. (2008) to be due to a late-L dwarf. Burleigh et al. (2006) determined that in an 11 ks long *Swift* observation SDSS 1212 had a count rate of 2.6×10^{-3} cts/s. They fitted the *Swift* X-ray spectrum with various one-temperature models, but the accretion mechanism (wind vs. Roche lobe) could not be established. The photon statistics were also insufficient for studying the X-ray light curve.

Here we report on an *XMM-Newton* observation of SDSS 1212 from which we unambiguously confirm that it is an accreting WDL system. We derive an improved estimate for its mass accretion rate and discuss the result in the framework of evolutionary scenarios for this system.

2. XMM-Newton observations and analysis

XMM-Newton observed SDSS 1212 on 6 June 2015 for 22 ks (Obs-ID 0760440101) with all EPIC instruments using the THIN filter and with the Optical Monitor (OM) in FAST MODE using the B band filter.

We restrict the analysis to EPIC/pn, which provides the highest sensitivity of the EPIC detectors. The data analysis was carried out with *XMM-Newton*’s Standard Science Analysis System (SAS) version 15.0.0. The observation is not affected by flaring particle background, therefore we used the full exposure time of 22 ks for the analysis. We filtered the data for pixel patterns ($0 \leq \text{PATTERN} \leq 12$), quality flag (FLAG = 0), and events channels ($200 \leq \text{PI} \leq 15\,000$). Source detection was performed in three energy bands: 0.2–1.0 keV (S), 1.0–2.0 keV (M), and 2.0–12.0 keV (H) using a customized procedure based on the steps implemented in the SAS task EDETECT_CHAIN. The net EPIC/pn source count rates are given in Table 1. We note that SDSS 1212 is also detected in the MOS cameras at a net count rate of 0.0167 ± 0.0010 cts/s and 0.0178 ± 0.0010 cts/s in the broad band for MOS 1 and MOS 2, respectively.

For the spectral and temporal analysis we allowed only pixel patterns with FLAG ≤ 4 . We defined a circular photon extraction region with radius of $30''$ centred on the EPIC/pn source position. The background was extracted from an adjacent circular region with radius of $45''$ on the same CCD chip. The background

Table 1. X-ray count rate and pulsed fraction ($PF_{\text{ sine}}$) from a sine fit for EPIC/pn data in different energy bands.

Energy [keV]	Band label	Net source rate [cts/s]	$PF_{\text{ sine}}$
0.2–12.0	B	0.0615 ± 0.0021	1.0
0.2–1.0	S	0.0323 ± 0.0015	0.94 ± 0.03
1.0–2.0	M	0.0188 ± 0.0012	0.93 ± 0.05
2.0–12.0	H	0.0104 ± 0.0009	1.0

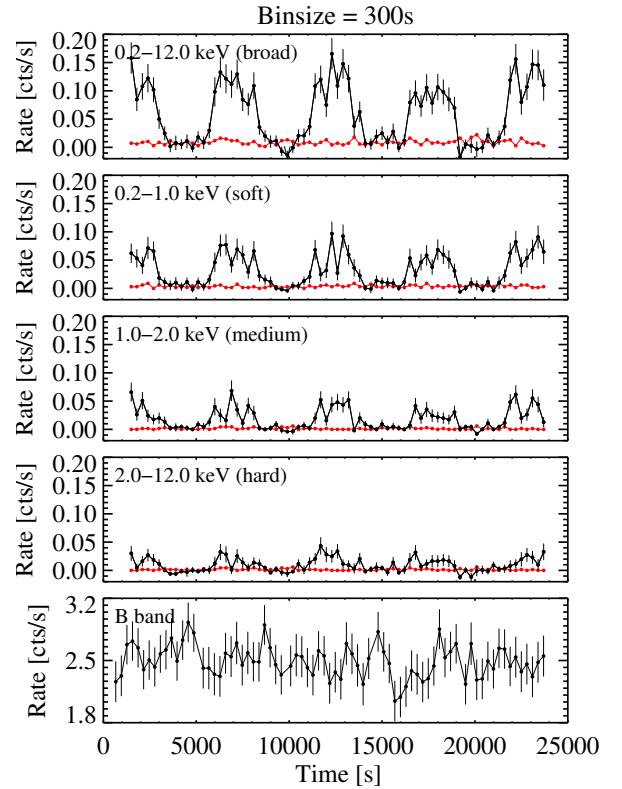


Fig. 1. OM B -band light curve and EPIC/pn X-ray light curve of SDSS 1212 with 1σ errors in four energy bands as labelled in the upper left of each panel. X-ray light curves represent the background-subtracted source signal (black) and for comparison the background signal (red). The bin size is 300 s.

subtraction of the light curve was carried out with the SAS task EPICLCCORR, which also corrects for instrumental effects. We then barycentre-corrected the photon arrival times using the SAS tool BARYCEN.

The light curve shows a clear periodic modulation in all energy bands with larger amplitude for softer emission (Fig. 1). The modulation does not appear to be sinusoidal, displaying on-off behaviour that is typical of strongly magnetized accreting WDs or AM Her systems (Cropper 1990). In the minimum the counts drop to zero, suggesting that the area of accretion, the pole cap, is completely occulted by the WD. All energy bands show flickering typical of X-ray emission from CVs. Lomb-Scargle periodogram analysis of the broad band (0.2–12 keV) light curve yields a period of $P_{\text{ orb}} = 88.3 \pm 0.6$ min. This value and its 1σ error were derived with a bootstrap approach from 5000 simulated broad band light curves drawn randomly from the count rates and errors. This period is in good agreement with published periods for the H α emission (93.6 ± 14.4 min; Schmidt et al. 2005), the near-IR photometry

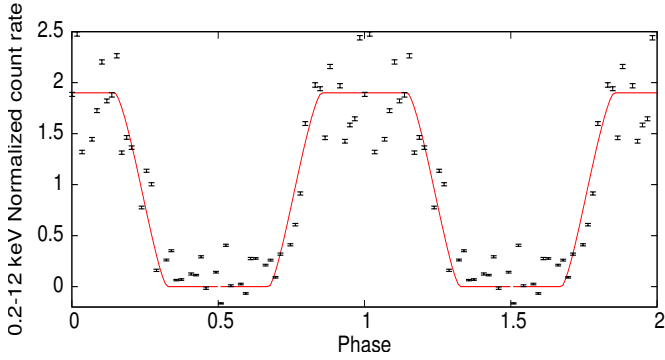


Fig. 2. Barycentre-corrected X-ray (EPIC/pn 0.2–12 keV) light curve of SDSS 1212 folded using the ephemeris of Burleigh et al. (2006) and the period determined from the X-ray signal. The bin size is 450 s. The best-fit model is shown in red.

(87.84 ± 1.44 min; Debes et al. 2006), and the optical photometry (88.428 ± 0.001 min; Burleigh et al. 2006).

To first approximation we fitted a sinusoid to the light curve from which we determined the pulsed fraction (PF) taking into account the uncertainties on y -offset and amplitude of the sine curve. The values obtained for the individual energy bands (see Table 1) are consistent with the 100% PF observed in polars.

The phase-folded X-ray light curve of SDSS 1212 is displayed in Fig. 2 together with a geometric model based on the one presented by Wynn & King (1992) and Brinkworth et al. (2004), which describes direct accretion from a donor onto a WD magnetosphere with a post-shock region characterized through the angle between magnetic and rotation axis (m), the pole-cap opening half-angle (b), and the system inclination (i). We ran the model over a range of parameter space to determine the likely values for these angles, assuming a single pole to be responsible for the variation. The modelling was performed on the X-ray light curve with a bin size of 150 s. We found $80^\circ \gtrsim i \gtrsim 70^\circ$, $110^\circ \gtrsim m \gtrsim 100^\circ$, and $b \approx 30^\circ$. These values meet the criteria for the self-occultation as in Wynn & King (1992) and references therein. We confirmed the size of the accretion region using different binnings with lower time-resolution. We also explored the effects of a vertical extent of the column up to $1 R_{WD}$ obtaining an upper limit of $0.2 R_{wd}$ and no major effect on the values of the other parameters. A small vertical extent of the emission region is also suggested by the fact that the flux drops to zero and the ingress and the egress are steep.

The EPIC/pn spectrum of SDSS 1212 was first fitted with single-component models: a power law, a black body, or an optically thin model, none of which adequately describes the spectral shape. When we add a simple absorber (TBABS) and leave the abundance free to vary, the thermal APEC model provides a reasonable fit. However, the 90% confidence level of the abundance is compatible with zero, which is an unphysical result (see Table 2). We also tested representations with two spectral components. In particular, the spectrum is compatible with an absorbed two-temperature ($2T$) thermal model [TBABS · (APEC + APEC)], which yields a better χ^2_{red} than the one-temperature ($1T$) model. However, similar to the case of the $1T$ -model, the abundance cannot be constrained by the fit. If, in turn, the abundance is fixed to the value obtained from the $1T$ -model, the additional low-temperature component turns out to be completely unconstrained. We conclude that the observed spectrum does not provide information on a possible multi-temperature environment. There is therefore no evidence for an additional lower temperature blackbody component such as the one typically used

Table 2. Best-fit parameters for the EPIC/pn spectrum of SDSS 1212 and values corresponding to upper and lower 90% confidence ranges.

χ^2_{red} (d.o.f.)	TBABS · APEC		
	N_H [cm^{-2}]	kT [keV]	Z [Z_\odot]
1.13(22)	$2.3^{5.1}_{0.0} \times 10^{20}$	$2.62^{3.58}_{1.99}$	$0.11^{0.44}_{0.0}$

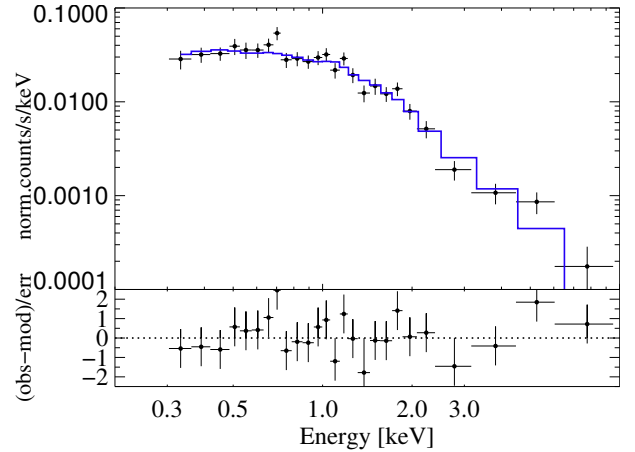


Fig. 3. Time-averaged EPIC/pn X-ray spectrum of SDSS 1212 with best-fitting one-temperature APEC model (solid blue line) and residuals.

to represent a soft excess in X-ray spectra of polars and intermediate polars ($\ll 0.1$ keV, see e.g. Beuermann et al. 2012; Bernardini et al. 2012). Such a component would also be physically unacceptable as it would be locally super-Eddington.

We show in Fig. 3 the observed EPIC/pn spectrum together with the $1T$ -model. The total galactic absorption in the direction of SDSS 1212 is $\sim 2 \times 10^{20} \text{ cm}^{-2}$ (Dickey & Lockman 1990), consistent with the value determined for the EPIC/pn spectrum. Given the distance of 120 pc (Burleigh et al. 2006), the intrinsic absorption of the source must be very low.

The X-ray flux is $1.5 \times 10^{-13} \text{ erg/cm}^2/\text{s}$, taking into account the bolometric correction to the 0.001–100 keV range, and $1.3 \times 10^{-13} \text{ erg/cm}^2/\text{s}$ for the 0.2–12 keV range. This latter value is similar to the value obtained by Burleigh et al. (2006) from the *Swift* spectrum ($1.2 \times 10^{-13} \text{ erg/cm}^2/\text{s}$) for an absorbed $1T$ fit. Despite the low statistics of the *Swift* data, these measurements, taken about one decade apart, indicate that the X-ray source is rather stable in time. With the distance ($d = 120$ pc) from Burleigh et al. (2006), we determine the bolometric X-ray luminosity to $\log L_x [\text{erg/s}] = 29.4$. From the X-ray luminosity we derive a mass accretion rate of $\dot{M}_{acc} \sim 2.6 \times 10^{-14} M_\odot/\text{yr}$; where we have used a slightly higher WD mass than Burleigh et al. (2006; $0.8 M_\odot$; see Sect. 3 for a justification) and a correspondingly smaller radius ($R_{WD} = 7 \times 10^8 \text{ cm}$). This value for \dot{M}_{acc} only includes the kinetic energy converted into X-ray luminosity. The value is higher when contributions from cyclotron emission and luminosity of the hot spot are considered.

The X-ray count rate in the minimum of the light curve ($0.35 \leq \phi \leq 0.65$) is 0.0046 cts/s with a standard deviation of 0.0086 cts/s. This corresponds to an upper limit of the X-ray luminosity. With the count-to-flux conversion factor derived from the time-averaged X-ray spectrum, we obtain $\log L_{x,min} [\text{erg/s}] = 27$. This value can be understood to represent the upper limit to any possible residual emission.

B-band photometry acquired with the OM in FAST MODE, simultaneously with the X-ray observations, was extracted with the SAS task OMCHAIN, and the time series was barycentre corrected. A Lomb-Scargle periodogram analysis did not yield a significant periodicity, and when folded on the X-ray period, no phase-related variability is seen (Fig. 1, lowest panel). At the time of the OM observation, SDSS 1212 was at $B_{\text{OM}} = 18.28 \pm 0.08$ mag, which is consistent with the SED provided by Debes et al. (2006) and with the u' and g' photometry shown by Burleigh et al. (2006). The optical light curve presented by Burleigh et al. (2006) showed only a weak modulation ($\lesssim 10\%$ in u' and $\sim 4\%$ in g'). Given the low statistics of the OM data, it is therefore not surprising that no significant variability is detected in our *B*-band light curve.

3. Discussion

To date, only four period-bounce candidates have infrared detections: EF Eri (Schwope et al. 2007), SDSS J 143317.78+101123.3 (Littlefair et al. 2013; Hernández Santisteban et al. 2016), WZ Sge (Harrison 2016), and SDSS 1212 (Farihi et al. 2008). SDSS J 1433+1011 and WZ Sge are non-magnetic CVs, while EF Eri has been the textbook example for a LARP, but is also considered a candidate period bouncer (Schwope et al. 2007; Schwope & Christensen 2010). The X-ray luminosity of EF Eri (2×10^{29} erg/s; see Schwope et al. 2007) is remarkably similar to our measurement for SDSS 1212. However, no X-ray variability has been detected for EF Eri during its extended low state, implying that accretion (almost) stopped. Our detection of X-ray orbital modulation in SDSS 1212, consistent with its binary period found with other methods, provides unambiguous proof for accretion from the L dwarf onto the WD and establishes this system as a new benchmark for interacting binaries consisting of a WD and a substellar companion with low accretion rates.

The X-ray luminosity of SDSS 1212, both during our *XMM-Newton* observation in 2015 and during the *Swift* observation nine years before, is several orders of magnitude higher than that of any single L dwarf ($< 10^{26}$ erg/s; see Audard et al. 2007, and the compilation by Cook et al. 2014), clearly ruling out coronal emission from the ultracool companion. Together with its orbital modulation, the high X-ray luminosity of SDSS 1212 therefore is another clear piece of evidence for accretion onto the magnetized WD.

Following the lines of argument in Webbink & Wickramasinghe (2005), the mass flux driven by coronal X-ray emission from an L dwarf with an assumed $\log L_x$ [erg/s] ~ 25 would be $10^{-16} M_{\odot}/\text{yr}$ at most. The detection of winds from late-type stars requires high-resolution UV spectroscopy and is at present not possible for L dwarfs. A very small number of late-type stars have measured wind accretion rates, including two M dwarfs that show much smaller \dot{M}_w than expected from the empirical \dot{M}_w vs. F_x relation for solar-type stars (Wood et al. 2015). Extrapolating from that relation to low F_x , for an adopted $\log L_x$ [erg/s] ~ 25 for the L dwarf, its wind would be $\approx 10^{-17} M_{\odot}/\text{yr}$, making it difficult to provide the observed accretion rate of SDSS 1212 (considering that we measured a lower limit of $3 \times 10^{-14} M_{\odot}/\text{yr}$). This leaves Roche-lobe overflow as the most likely origin for the mass transfer.

Farihi et al. (2008) estimated the L-dwarf radius as $0.09 R_{\odot}$ and calculated the Roche lobe to be $R_L = 0.11 R_{\odot}$. However, this is based on the assumption that the WD mass is $0.6 M_{\odot}$, a value typical of a non-magnetic, isolated WD. There is evidence

that WDs in CVs have higher masses than single WDs and those in detached systems (Zorotovic et al. 2011). Moreover, single magnetic WDs have also been found to be more massive than non-magnetic WDs (Ferrario et al. 2015). Considering that the non-magnetic CV SDSS 1433+1011 – with an L-dwarf companion – has a mass of $0.868 M_{\odot}$ (Littlefair et al. 2008; Hernández Santisteban et al. 2016), assuming a mass of $\sim 0.8 M_{\odot}$ for SDSS 1212 is therefore plausible. For this value, using Eq. (5) from Breedt et al. (2012), we determine $R_L = 0.10 R_{\odot}$, which is closer to the L-dwarf radius. Our detection of accretion, and thus the presence of an X-ray emitting region on the WD, also provides an explanation for the $H\alpha$ emission previously observed from SDSS 1212, as due to irradiation of the donor by the X-ray emission from the accreting WD. As a result of the irradiation the L dwarf may be inflated, making Roche-lobe filling even more likely.

To conclude, SDSS 1212 presents the characteristics of the long-sought class of period-bounce CVs (cool WD, substellar donor mass, and weak accretion), and it is located in the observationally still nearly unpopulated “boomerang” region of CV evolution models (e.g. Howell et al. 2001) that awaits observational confirmation. SDSS 1212 is the first WLDL binary found to exhibit clear accretion-induced X-ray variability at a very low accretion rate. The WLDL binary EF Eri has long been known to show X-ray orbital modulation during high states (e.g. Patterson et al. 1981), but in its current low state the X-ray emission could not be found to be modulated at the WD spin/binary orbit (Schwope et al. 2007).

The X-ray orbital modulation of SDSS 1212 suggests that accreting WLDL systems may be easy to identify in the X-ray band through the magnetically confined accretion flow onto the polar regions of the WD. Sensitive searches for X-rays from WLDL binaries can therefore be expected to provide further examples of pulsed emission, ensuing determination of mass accretion rates at very weak levels, and the characterization of the multi-wavelength properties of the so far widely elusive class of period-bounce CVs.

Acknowledgements. D.D.M. acknowledges financial support from ASI INAF I/037/12/0. S.L.C. acknowledges support from the University of Leicester College of Science and Engineering.

References

- Audard, M., Osten, R. A., Brown, A., et al. 2007, *A&A*, 471, L63
- Bernardini, F., de Martino, D., Falanga, M., et al. 2012, *A&A*, 542, A22
- Beuermann, K., Burwitz, V., & Reinsch, K. 2012, *A&A*, 543, A41
- Breedt, E., Gänsicke, B. T., Girven, J., et al. 2012, *MNRAS*, 423, 1437
- Brinkworth, C. S., Burleigh, M. R., Wynn, G. A., & Marsh, T. R. 2004, *MNRAS*, 348, L33
- Burleigh, M. R., Marsh, T. R., Gänsicke, B. T., et al. 2006, *MNRAS*, 373, 1416
- Caswell, S. L. 2014, *Mem. Soc. Astron. It.*, 85, 731
- Cook, B. A., Williams, P. K. G., & Berger, E. 2014, *ApJ*, 785, 10
- Cropper, M. 1990, *Space Sci. Rev.*, 54, 195
- Debes, J. H., López-Morales, M., Bonanos, A. Z., & Weinberger, A. J. 2006, *ApJ*, 647, L147
- Dickey, J. M., & Lockman, F. J. 1990, *ARA&A*, 28, 215
- Farihi, J., Burleigh, M. R., & Hoard, D. W. 2008, *ApJ*, 674, 421
- Ferrario, L., de Martino, D., & Gänsicke, B. T. 2015, *Space Sci. Rev.*, 191, 111
- Gänsicke, B. T., Dillon, M., Southworth, J., et al. 2009, *MNRAS*, 397, 2170
- Harrison, T. E. 2016, *ApJ*, 816, 4
- Hernández Santisteban, J. V., Knigge, C., Littlefair, S. P., et al. 2016, *Nature*, 533, 366
- Howell, S. B., Nelson, L. A., & Rappaport, S. 2001, *ApJ*, 550, 897
- Knigge, C., Baraffe, I., & Patterson, J. 2011, *ApJS*, 194, 28
- Littlefair, S. P., Dhillion, V. S., Marsh, T. R., et al. 2008, *MNRAS*, 388, 1582

- Littlefair, S. P., Savoury, C. D. J., Dhillon, V. S., et al. 2013, *MNRAS*, **431**, 2820
- Marcy, G. W., & Butler, R. P. 2000, *PASP*, **112**, 137
- Nordhaus, J., & Spiegel, D. S. 2013, *MNRAS*, **432**, 500
- Patterson, J., Williams, G., & Hiltner, W. A. 1981, *ApJ*, **245**, 618
- Rebassa-Mansergas, A., Schreiber, M. R., & Gänsicke, B. T. 2013, *MNRAS*, **429**, 3570
- Schmidt, G. D., Szkody, P., Silvestri, N. M., et al. 2005, *ApJ*, **630**, L173
- Schmidt, G. D., Szkody, P., Henden, A., et al. 2007, *ApJ*, **654**, 521
- Schwöpe, A. D., & Christensen, L. 2010, *A&A*, **514**, A89
- Schwöpe, A. D., Brunner, H., Hambaryan, V., & Schwarz, R. 2002, in *The Physics of Cataclysmic Variables and Related Objects*, eds. B. T. Gänsicke, K. Beuermann, & K. Reinsch, *ASP Conf. Ser.*, **261**, 102
- Schwöpe, A. D., Staude, A., Koester, D., & Vogel, J. 2007, *A&A*, **469**, 1027
- Schwöpe, A. D., Nebot Gomez-Moran, A., Schreiber, M. R., & Gänsicke, B. T. 2009, *A&A*, **500**, 867
- Stelzer, B., Micela, G., Flaccomio, E., Neuhäuser, R., & Jayawardhana, R. 2006, *A&A*, **448**, 293
- Webbink, R. F., & Wickramasinghe, D. T. 2005, in *The Astrophysics of Cataclysmic Variables and Related Objects*, eds. J.-M. Hameury, & J.-P. Lasota, *ASP Conf. Ser.*, **330**, 137
- West, A. A., Hawley, S. L., Walkowicz, L. M., et al. 2004, *AJ*, **128**, 426
- Wood, B. E., Linsky, J. L., & Güdel, M. 2015, in *Characterizing Stellar and Exoplanetary Environments*, eds. H. Lammer, & M. Khodachenko, *Astrophys. Space Sci. Lib.*, **411**, 19
- Wynn, G. A., & King, A. R. 1992, *MNRAS*, **255**, 83
- Zorotovic, M., Schreiber, M. R., & Gänsicke, B. T. 2011, *A&A*, **536**, A42